Electronic Supplementary Material (ESI) for Dalton Transactions.

Supporting Information:

Molecular and Electronic Structure of the Dithiooxalato Radical Ligand Stabilised by Rare Earth Coordination

Jake McGuire, Bradley Wilson, James McAllister, Haralampos N. Miras, Claire Wilson, Stephen Sproules and Joy H. Farnaby**

WestCHEM School of Chemistry, University of Glasgow, Glasgow G12 8QQ (UK)

Email: stephen.sproules@glasgow.ac.uk; joy.farnaby@glasgow.ac.uk

Contents

Experimental

Synthesis. All air-sensitive manipulations were carried out in an MBraun glovebox or using standard Schlenk techniques. All glassware was dried at 130 °C overnight prior to use. Filter cannulas were prepared using Whatman 25 mm glass microfiber filters and were pre-dried at 130 °C overnight. Dry solvents (CH_2Cl_2, MeCN, toluene) were obtained using an Innovative Technology Inc. Pure Solv 400-5-MD solvent purification system (activated alumina columns). Solvents were sparged with N_2 and stored in ampoules over molecular sieves. The compounds $CoCp_2$,[1] $K_2[Ni(dto)_2]$,[2] and $[PPh_4]_2[Ni(dto)_2]$,[3] were prepared according to literature procedures. All other reagents were used as received.

$[Ni\{(dto)YTp_2\}_2]$ (1). Colourless solutions of KTp (100 mg; 0.397 mmol, 4 eqv) in H_2O (5 mL) and anhydrous YCl_3 (39 mg; 0.20 mmol, 2 eqv) in H_2O (5 mL) were simultaneously added dropwise, with stirring, to a dark purple solution of $K_2[Ni(dto)_2]$ (37 mg; 0.10 mmol, 1 eqv) in H_2O (10 mL) resulting in the immediate formation of a light-violet precipitate. After 5 minutes the suspension was cooled from RT to 2 °C and left for 12 h. The precipitate was collected on a Gooch crucible and was washed with H_2O (3 × 5 mL), Et_2O (3 × 5 mL) and dried *in vacuo* yielding $[Ni\{(dto)YTp_2\}_2]$ **1** (98 mg, 0.07 mmol, 70%).

Anal. Calcd. for $C_{40}H_{40}B_4N_{24}NiO_4S_4Y_2$: C, 36.15; H, 3.03; N 25.03. Found: C, 36.29; H, 3.12; N, 25.15%. ATR-IR (ν / cm^{-1}): ν(B–H) 2457 w, ν(C–N) 1538 s, ν(C–O) 1523 s, ν(C–O) 1504 s, 1409 s, 1403 m, 1297 m, 1212 m, 1130 m, 1044 s, ν(CCS) 979 m. ^1H NMR (C_6D_6; δ / ppm): 7.34 (br d, 12H, pyrazolyl-CH), 7.09 (br d, 12H, pyrazolyl-CH), 5.68 (br t, 12H, pyrazolyl-CH), 4.68 (br s, BH). ^{13}C NMR (C_6D_6; δ / ppm): 200.91 (s), 141.23 (s), 135.33 (s), 104.65 (s). Absorption spectrum (CH_2Cl_2; λ_{max} / nm (ε / 10^4 M^{-1} cm^{-1})): 525 (sh, 0.23), 549 (0.28), 592 (0.39), 620 (sh, 0.25).

$[Ni\{(dto)GdTp_2\}_2]$ (2). Compound **2** was synthesised in a manner analogous to **1** using $K_2[Ni(dto)_2]$ (37 mg; 0.10 mmol, 1 eqv), $GdCl_3{\cdot}6H_2O$ (74 mg; 0.20 mmol, 2 eqv) and KTp (100 mg, 0.40 mmol, 4 eqv) and was isolated as a light-violet solid $[Ni\{(dto)GdTp_2\}_2]$ **2** (190 mg, 0.065 mmol, 65%).

Anal. Calcd. for $C_{40}H_{40}B_4CoN_{24}NiO_4S_4Gd_2$: C, 32.78; H, 2.75; N, 22.94. Found: C, 33.02; H, 2.68; N, 23.09. ATR-IR (ν / cm^{-1}): ν(B–H) 2461 w, ν(C–N) 1535 s, ν(C–O) 1519 s, ν(C–O) 1503 s, 1403 m, 1300 m, 1225 m, 1125 m, 1049 s, ν(CCS) 976 m. Absorption spectrum (CH_2Cl_2; λ_{max} / nm (ε / 10^4 M^{-1} cm^{-1})): 525 (sh, 0.22), 552 (0.28), 592 (0.39), 620 (sh, 0.24).

$[CoCp_2]^+[Ni\{(dto)YTp_2\}_2]^{-\bullet}$ (3). With stirring, a purple solution of **1** (60 mg; 0.05 mmol, 1 eqv) in toluene (10 mL) was treated dropwise with a dark brown solution of $CoCp_2$ (10 mg; 0.05 mmol, 1 eqv) in toluene (5 mL) over 2 minutes, resulting in the formation a teal precipitate. The suspension was stirred for 15 minutes. The precipitate was collected on a Gooch crucible and then washed with toluene (3 × 5 mL) and dried *in vacuo* yielding $[CoCp_2]^+[Ni\{(dto)YTp_2\}_2]^{-\bullet}$ **3** (42 mg, 0.03 mmol, 30%).

Anal. Calcd. for $C_{50}H_{50}B_4CoN_{24}NiO_4S_4Y_2$: C, 39.56; H, 3.32; N, 22.14. Found: C, 39.40; H, 3.22; N, 22.24. Absorption spectrum (CH_2Cl_2; λ_{max} / nm (ε / 10^4 M^{-1} cm^{-1})): 556 (sh, 0.35), 595 (0.42), 622 (sh, 0.31), 710 (sh, 0.11), 1110 (0.01), 1320 (0.02), 1790 (0.13).

$[CoCp_2]^+[Ni\{(dto)GdTp_2\}_2]^{-\bullet}$ (4). This compound was synthesised in a manner analogous to **3**, using **2** (30 mg; 0.02 mmol, 1 eqv) and $CoCp_2$ (4 mg; 0.02 mmol, 1 eqv), and was isolated as a teal solid, $[CoCp_2]^+[Ni\{(dto)GdTp_2\}_2]^{-\bullet}$ **4** (14 mg, 0.008 mmols, 40%).

Anal. Calcd. for $C_{50}H_{50}B_4CoN_{24}NiO_4S_4Gd_2$: C, 36.29; H, 3.05; N, 20.32. Found: C, 36.36; H, 2.97; N, 20.17. Absorption spectrum (CH_2Cl_2; λ_{max} / nm (ε / 10^4 M^{-1} cm^{-1})): 556 (sh, 0.31), 595 (0.39), 622 (sh, 0.31), 710 (sh, 0.11), 1110 (0.01), 1320 (0.02), 1790 (0.13).

$[PPh_4]_2[Ni\{(dto)SnCl_4\}_2]$ (5). A 50 mL Schlenk flask was charged with a red-pink solution of $[PPh_4]_2[Ni(dto)_2]$ (98 mg; 0.10 mmol) in CH_2Cl_2 (8 mL) and treated dropwise (0.05 mL aliquots over 30 seconds), while constantly stirring, with 1.0 M $SnCl_4$ in CH_2Cl_2 (0.20 mL; 0.20 mmol) *via* syringe to give an immediate colour change from red-pink to deep blue. Stirring was continued for 10 minutes, and then the mixture was layered with hexanes (16 mL) and left standing overnight at RT. A dark indigo solid was collected by cannula filtration and washed with hexanes (3 × 10 mL). The solid was subsequently dried *in vacuo* to yield a microcrystalline solid of $[PPh_4]_2[Ni\{(dto)SnCl_4\}_2]$ **5** (82 mg, 0.05 mmol, 54%).

Anal. Calcd. for $C_{52}H_{40}Cl_8NiO_4P_2S_4Sn_2$: C, 41.67; H, 2.69. Found: C, 41.79; H, 2.61. ATR-IR (ν / cm^{-1}): 2361 w, 1629 w, 1581 w, ν(C–O) 1493 s, ν(C–O) 1479 s, ν(PPh_4) 1435 s, 1106 s, ν(CCS) 995 m. ^1H NMR (CD_2Cl_2; δ / ppm): 7.92 (m, 4H, PPh_4^+), 7.76 (m, 8H, PPh_4^+), 7.62 (m, 8H, PPh_4^+). ^{13}C NMR (CD_2Cl_2; δ / ppm): 209.73 (s), 136.20 (s), 134.88 (s), 131.11 (s), 117.93 (d, J_{CP} = 86.60 Hz). Absorption spectrum (CH_2Cl_2; λ_{max} / nm (ε / 10^4 M^{-1} cm^{-1})): 544 (0.22), 582 (0.31), 622 (0.44), 655 (sh, 0.25).

X-ray Crystallographic Data Collection and Structure Refinement

Single crystals suitable of X-ray diffraction were obtained by slow diffusion of diethyl ether into concentrated solutions of the compounds using dichloromethane (**1** and **2**) at 2 °C and acetonitrile (**3** and **4**) at RT. Crystals of **5** were grown from diffusion of hexane into a dichloromethane solution of the complex at -25 °C. The crystals were coated with paratone oil or Fomblin ® and mounted on a Mitegen MicroMount. Single-crystal structure data for **1**, **4** and **5** were collected using a Bruker D8 VENTURE diffractometer equipped with a Photon II CPAD detector, with an Oxford Cryosystems N-Helix device mounted on an IμS 3.0 (dual Cu and Mo) microfocus sealed tube generator. Data for **2** and **3** were collected using a Bruker SMART APEX CCD diffractometer equipped with a Kryoflex. Data were collected at 150 K using Mo-Kα radiation (λ = 0.71073 Å). Structure solution and refinement for all structures were carried out with SHELXT[4] and SHELXL-2018[5] either using the Olex2[6] or WinGX[7] software packages. Data collection and reduction were performed using the APEX3 or APEX2 programs. Corrections for incident and diffracted beam absorption effects were applied using empirical absorption corrections.[8] All non–hydrogen atoms were refined with anisotropic thermal parameters. Solvent molecule sites were found and included in the refinement of structure were generally refined with anisotropic thermal parameters. The positions of hydrogen atoms were calculated based on stereochemical considerations and and included as part of a riding model with isotropic ADPs at 1.2 Ueq of the parent atom. Final unit cell data and refinement statistics are collected in Table S1. The crystallographic data for compounds **1** – **5** (CCDC 1886429–1886430, 1889410, 1886431-1886432) can be obtained free of charge from the Cambridge Crystallographic Data Centre, 12, Union Road, Cambridge CB2 1EZ; fax: (+44) 1223-336-033, deposit@ccdc.cam.ac.uk.

Physical Methods

Electronic absorption spectra were collected using a Shimadzu UV-3600 UV/vis/NIR spectrophotometer. IR spectra were collected using either a Shimadzu IRAffinity-1S or a Shimadzu FTIR 8400S spectrophotometer. ^{1}H and ^{13}C NMR data were recorded on an AVIII 400 MHz instrument and were referenced internally to the residual solvent. X-band EPR spectra were collected on a Bruker ELEXSYS E500 spectrometer and simulations were performed using Bruker's Xsophe software package.[9] Cyclic voltammetry measurements were performed with a Metrohm Autolab P128 potentiostat. The electrode configuration consisted of a 2 mm glassy carbon working electrode, a platinum auxiliary electrode and a reference electrode consisting of $Ag/AgNO_3$ (0.01 M in MeCN) incorporated into a salt bridge containing supporting electrolyte (to minimize Ag^+ leakage). The measurement were collected using a 1 mM solution of **1** and **3** dissolved in 5:1 anisole/dichloromethane containing 0.2 M $[N(^{n}Bu)_4]PF_6$ as electrolyte. All reduction potentials are referenced versus the ferrocenium/ferrocene ($Fc^{+/0}$) couple. Microanalyses were performed at London Metropolitan University by Stephen Boyer.

Table S1 Crystallographic Data

compound	**1**·$2CH_2Cl_2$	**2**·$2CH_2Cl_2$	**3**·CH_3CN	**4**·CH_3CN	**5**
formula	$C_{42}H_{44}B_4Cl_4N_{24}NiO_4S_4Y_2$	$C_{42}H_{44}B_4Cl_4Gd_2N_{24}NiO_4S_4$	$C_{52}H_{53}B_4CoN_{25}NiO_4S_4Y_2$	$C_{52}H_{53}B_4CoGd_2N_{25}NiO_4S_4$	$C_{52}H_{40}Cl_8NiO_4P_2S_4Sn_2$
fw	1498.82	1635.50	1559.13	1695.81	1498.71
T, K	150(2)	150(2)	150(2)	150(2)	150(2)
λ, Å	0.71073	0.71073	0.71073	0.71073	0.71073
2θ range, deg	4.66–50.58	4.62–52.44	4.41–50.52	4.40–56.54	4.40–56.58
crystal system	triclinic	triclinic	monoclinic	monoclinic	monoclinic
space group	$P\bar{1}$	$P\bar{1}$	$P2_1/c$	$P2_1/c$	$P2_1/n$
a, Å	7.7805(7)	7.754(2)	21.452(3)	21.551(1)	7.5323(4)
b, Å	11.4660(9)	11.475(2)	18.321(3)	18.3268(9)	21.605 (1)
c, Å	17.794(1)	17.902(4)	18.014(3)	18.074(1)	17.984(1)
α, deg	79.227(3)	79.546(3)	90	90	90
β, deg	86.607(3)	86.774(3)	113.699(2)	113.674(2)	90.339(2)
γ, deg	72.168(3)	72.601(3)	90	90	90
V, Å^3	1484.5(2)	1494.7(5)	6483(2)	6537.7(7)	2926.6(3)
Z	1	1	4	4	2
ρ, g cm^{-3}	1.677	1.817	1.597	1.723	1.701
μ, mm^{-1}	2.637	2.887	2.504	2.728	1.771
crystal size, mm	0.20 × 0.07 × 0.02	0.10 × 0.08 × 0.02	0.18 × 0.12 × 0.10	0.22 × 0.19 × 0.02	0.42 × 0.06 × 0.02
colour, habit	purple plate	blue plate	blue block	green plate	blue lath
reflections collected	19317	16210	108563	67695	36852
independent data	5418	5327	13599	16204	7242
parameters / restraints	390 / 0	385 / 0	839 / 0	839 / 0	331 / 0
GoF^{a}	1.070	1.022	1.030	1.049	1.063
R1^{b,c} / wR2^{d,c}	0.0383 / 0.0934	0.0314 / 0.0426	0.0444 / 0.0868	0.0383 / 0.0902	0.0290 / 0.0646
R1^{b,e} / wR2^{d,e}	0.0466 / 0.0969	0.0592 / 0.0633	0.0960 / 0.1094	0.0642 / 0.1069	0.0420 / 0.0738
largest diff. peak, e	0.938	1.453	0.724	1.492	0.667
largest diff. hole, e	–0.509	–0.850	–0.496	–1.398	–0.393

[a] GoF = $\{\Sigma[w(F_o^2 - F_c^2)^2]/(n-p)\}^{1/2}$, where n = number of reflections and p is the total number of parameters refined. [b] R1 = $\Sigma||F_o| - |F_c||/\Sigma|F_o|$. [c] R indices for data cut off at $I > 2\sigma(I)$. [d] wR2 = $\{\Sigma[w(F_o^2 - F_c^2)^2]/\Sigma[w(F_o^2)^2]\}^{1/2}$, where $w = 1/[\sigma^2(F_o^2) + (aP)^2 + bP]$, $P = (F_o^2 + 2F_c^2)/3$. [e] R indices for all data

Additional Crystallographic Data:

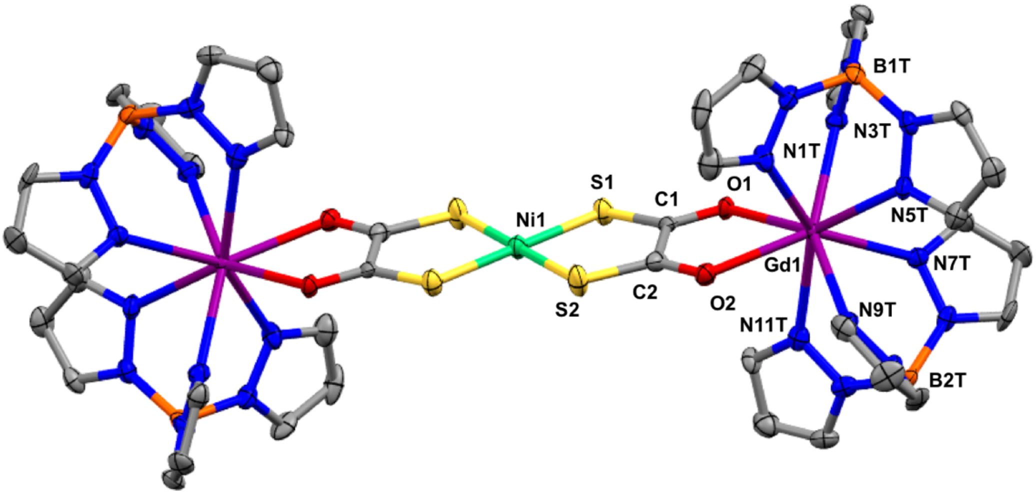

Fig. S1 Crystal structure of compound **2** with hydrogen atoms omitted for clarity and thermal ellipsoids drawn at 50% probability.

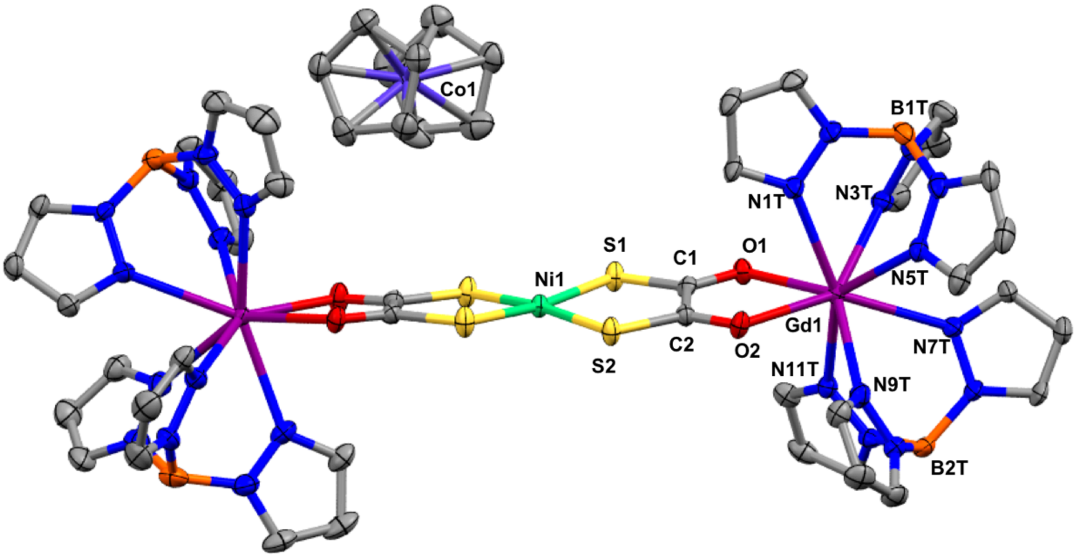

Fig. S2 Crystal structure of compound **4** with hydrogen atoms omitted for clarity and thermal ellipsoids drawn at 50% probability.

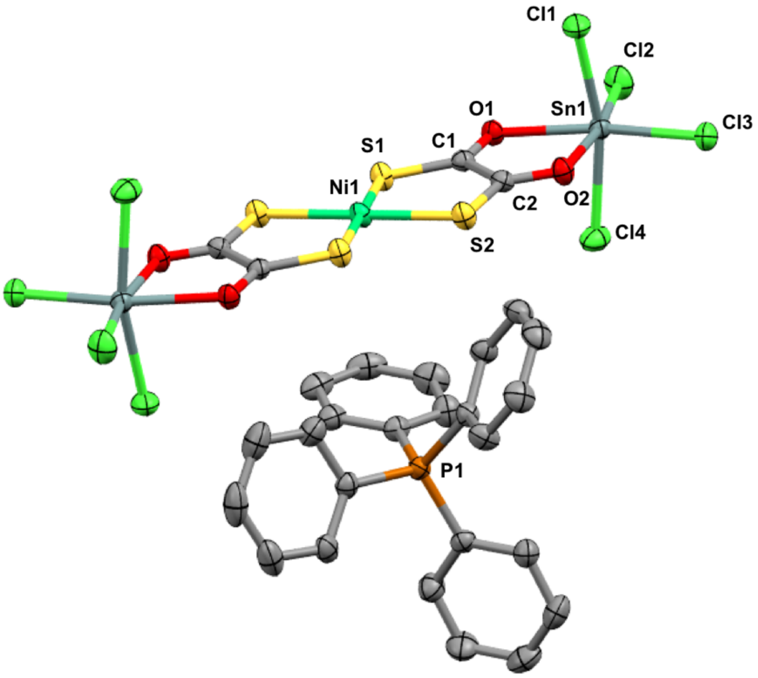

Fig. S3 Crystal structure of compound **5** with hydrogen atoms omitted for clarity and thermal ellipsoids drawn at 50% probability.

Spectroscopic Data for compounds 1-5 and $[PPh_4]_2[Ni(dto)_2]$:

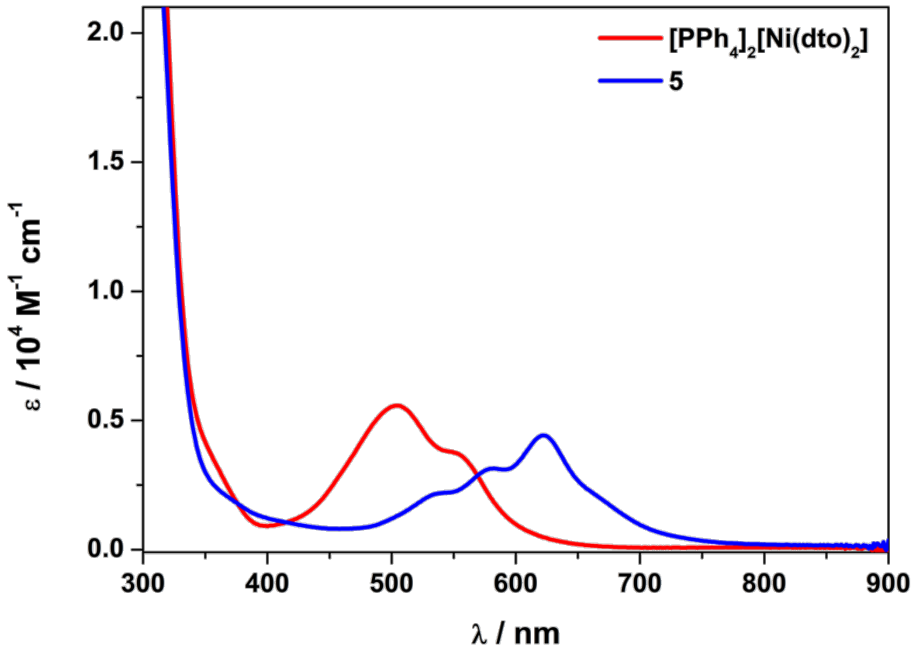

Fig. S4 Overlay of the electronic spectra of $[PPh_4]_2[Ni(dto)_2]$ and **5** recorded in CH_2Cl_2 solution at RT.

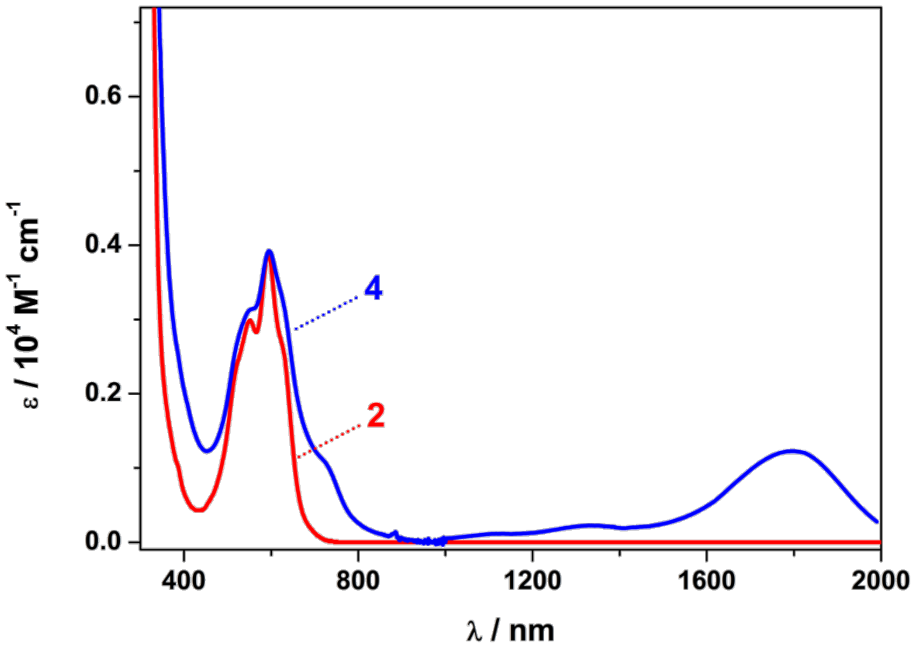

Fig. S5 Overlay of the electronic spectra of **2** and **4** recorded in CH_2Cl_2 solution at RT.

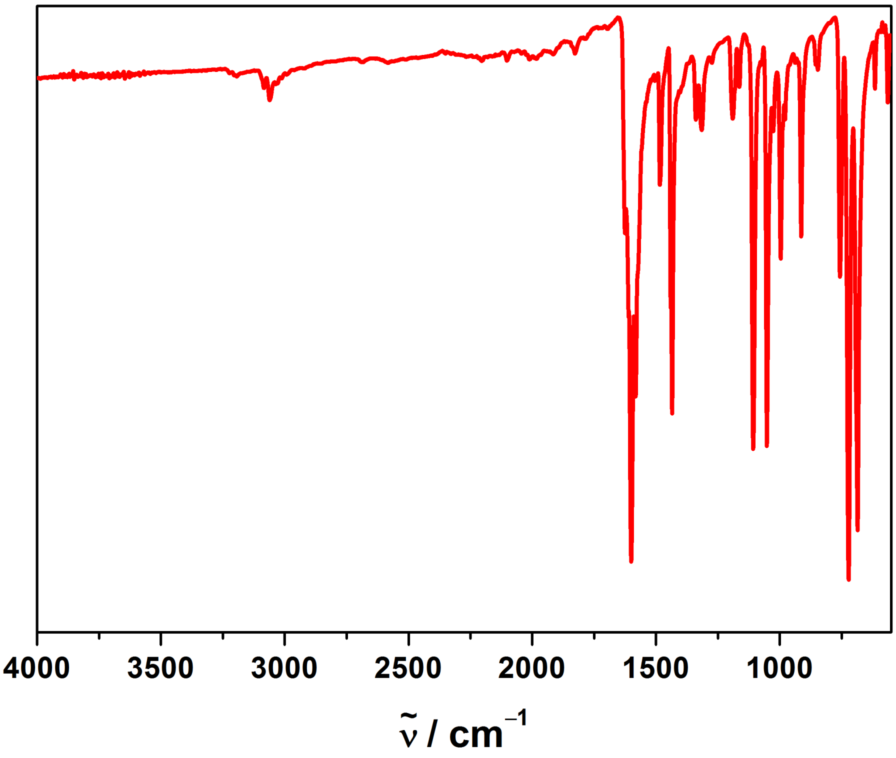

Fig. S6 ATR-IR spectrum of $[PPh_4]_2[Ni(dto)_2]$.

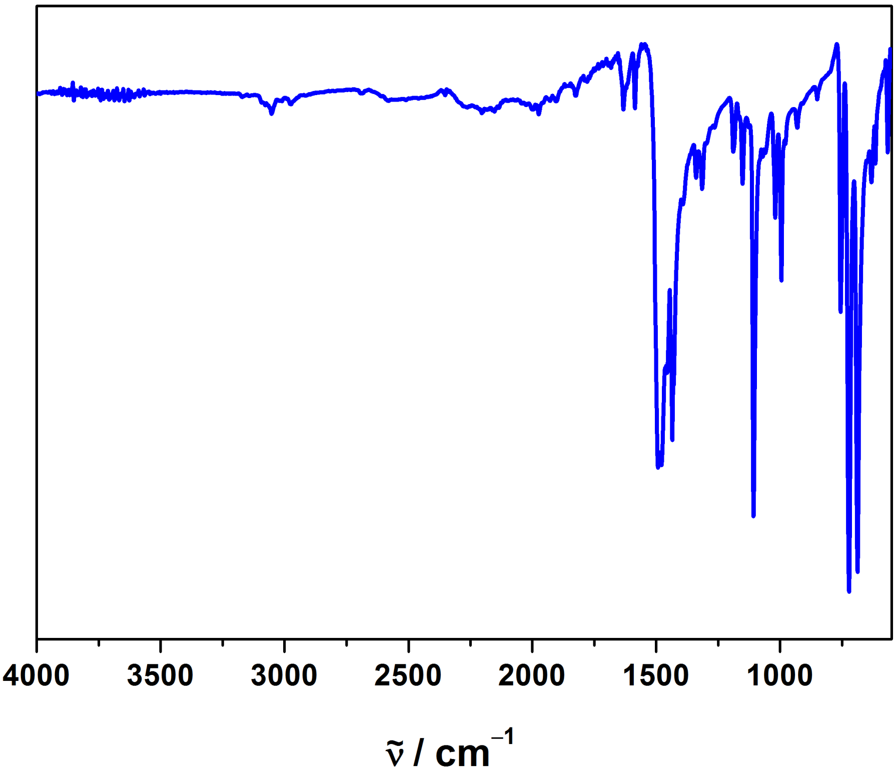

Fig. S7 ATR-IR spectrum of **5**.

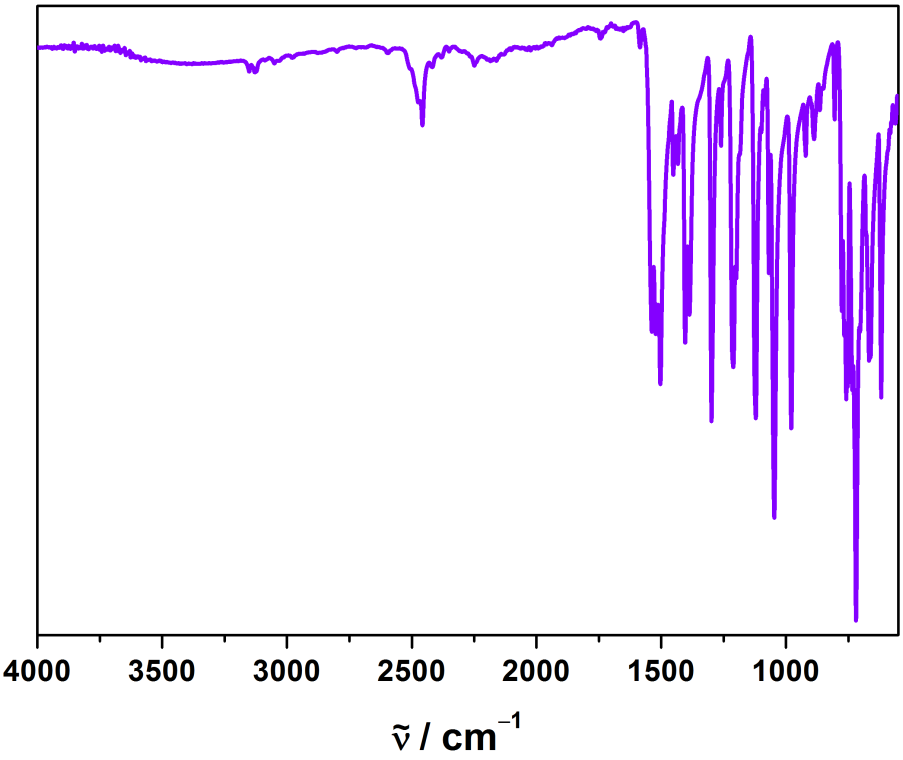

Fig. S8 ATR-IR spectrum of **1.**

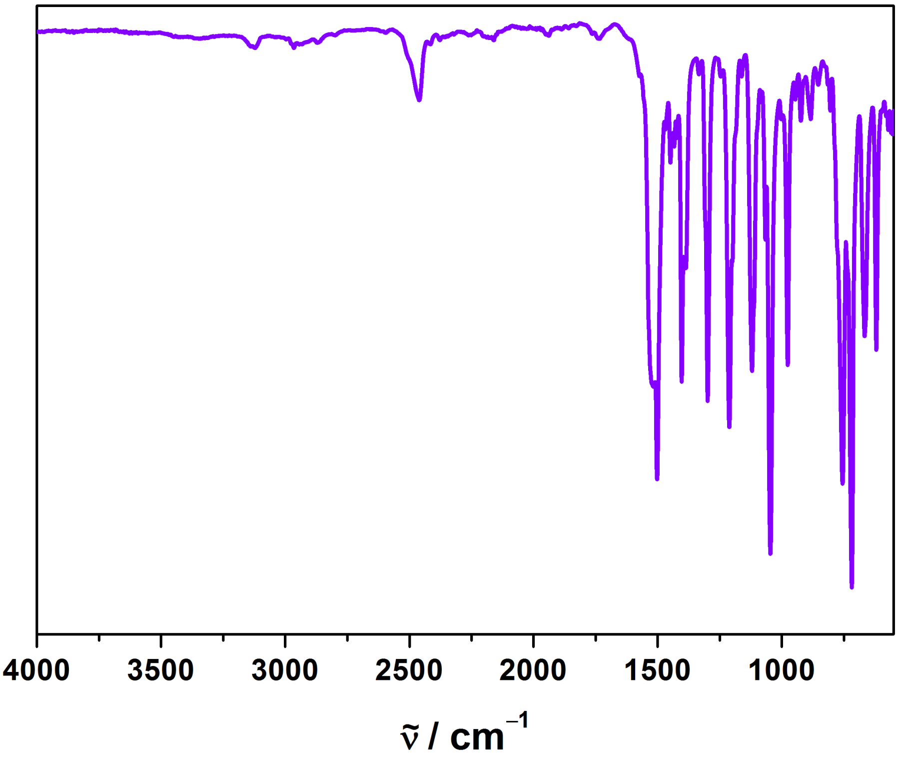

Fig. S9 ATR-IR spectrum of **2**.

Electrochemical Data for compound 2:

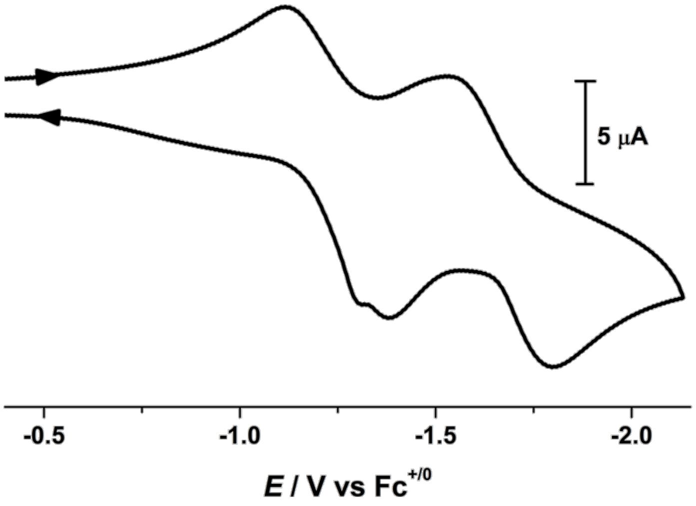

Fig. S10 Cyclic voltammogram of **2** in 5:1 anisole/CH_2Cl_2 solution (0.20 M $[N(^nBu)_4]PF_6$ supporting electrolyte) at 295 K at a scan rate of 100 mV s^{-1}. Potentials are referenced versus the Fc$^{+/0}$ couple.

EPR Data for compound 3:

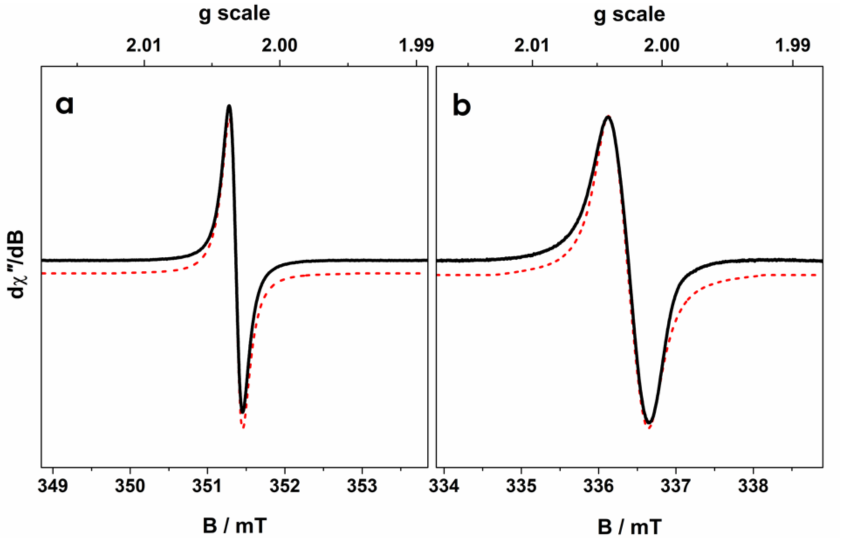

Fig. S11 X-band EPR spectra of **3** in (a) CH_2Cl_2 solution at 293 K (experimental conditions: frequency, 9.8518 GHz; power, 0.063 mW; modulation, 0.02 mT), and (b) CH_2Cl_2/MeCN at 130 K (experimental conditions: frequency, 9.42841 GHz; power, 0.63 mW; modulation, 0.01 mT). Experimental data are represented by the solid lines and simulations depicted by a dashed trace.

Calculations:

The program package ORCA was used for all calculations.[10] The geometry of of $[Ni\{(dto)SnCl_4\}_2]^{3-}$ was fully optimised using the BP86 functional,[11] employing the D3 dispersion correction[12] in and acetonitrile solvent with the conductor like screening model (COSMO).[13] The scalar relativistically recontracted def2-TZVP basis set was used for all atoms.[14] Auxiliary basis sets used to expand the electron density in the calculations were chosen to match the orbital basis. Electronic structures were calculated on crystallographic or optimised coordinates using the PBE0 hybrid functional.[15] The RIJCOSX algorithm was used to speed the calculation of Hartree–Fock exchange.[15,16] Increased integration accuracy (SPECIALGRIDINTACC 7) was used for metal atoms and sulfur. Calculations included the zeroth-order regular approximation (ZORA) for relativistic effects[17] as implemented by van Wüllen.[18] The self-consistent field calculations were tightly converged (1×10^{-8} E_h in energy, 1×10^{-7} E_h in the charge density, and 1×10^{-7} in the maximum element of the DIIS[19] error vector). The geometry was converged with the following convergence criteria: change in energy $<10^{-5}$ E_h, average force $<5 \times 10^{-4}$ E_h Bohr^{-1}, and the maximum force 10^{-4} E_h Bohr^{-1}. We used the broken symmetry (BS) approach to describe our computational results for **2** and **4**.[20] We adopt the following notation: the given system was divided into two fragments. The notation BS(m,n) refers then to a broken symmetry state with m unpaired α-spin electrons essentially on fragment 1 and n unpaired β-spin electrons localised on fragment 2. In most cases, fragments 1 and 2 correspond to the metal and the ligands, respectively. In this notation the standard high-spin, open-shell solution is written as BS($m + n$,0). The BS(m,n) notation refers to the initial guess to the wave function. The variational process does, however, have the freedom to converge to a solution of the form BS($m - n$,0) in which effectively the $n\beta$-spin electrons pair up with $n < m\alpha$-spin electrons on the partner fragment. Such a solution is then a standard $M_S \cong (m - n)/2$ spin-unrestricted Kohn-Sham solution. The exchange coupling constants J were calculated using Eq. 1,[21], assuming the spin-Hamiltonian Eq. 2 is valid.

$$J = \frac{E_{\mathrm{HS}} - E_{\mathrm{BS}}}{\langle \hat{S}^2 \rangle_{\mathrm{HS}} - \langle \hat{S}^2 \rangle_{\mathrm{BS}}} \tag{1}$$

$$\mathrm{J} = \frac{\mathrm{E_{HS}\text{-}E_{BS}}}{\langle \hat{\mathrm{S}}^2 \rangle_{\mathrm{HS}} \text{-} \langle \hat{\mathrm{S}}^2 \rangle_{\mathrm{BS}}} \hat{H} = -2J\hat{S}_{\mathrm{A}} \cdot \hat{S}_{\mathrm{B}} \tag{2}$$

Spin density plots were obtained using Molekel.[22]

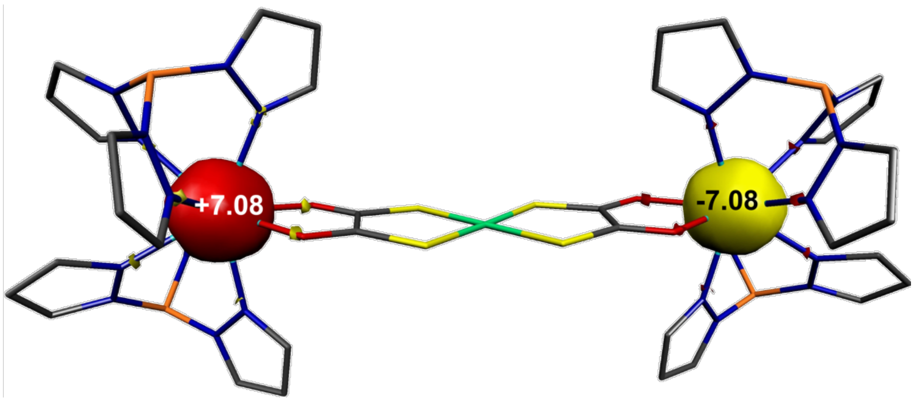

Fig. S12 Mulliken spin population analysis for **2** (red: α-spin; yellow: β-spin)

Table S2 Geometry Optimised Coordinates of $[Ni\{(dto)SnCl_4\}_2]^{3-}$

Ni	7.24220486735497	-0.00125928183015	-0.00038838104396
Sn	3.27227626859123	4.24559530888593	-0.31580885399695
Sn	11.21608648669772	-4.24430310132482	0.31625284495994
S	5.88687966851599	0.90083272922594	1.44052100787507
S	6.54544292094644	1.29129304937509	-1.60455178179268
S	8.59796483303221	-0.90287274156502	-1.44116735751390
S	7.93888608617029	-1.29391068592622	1.60373543354103
C	9.43872166513971	-2.09351491754809	-0.54620116191454
C	9.13315574790041	-2.27416893025212	0.87059537647200
C	5.04706766603047	2.09236844660285	0.54585531505234
C	5.35227513798697	2.27261936828200	-0.87108327682069
O	10.34312461087323	-2.84436792276738	-1.08950156370346
O	9.77878080225017	-3.17748258317036	1.53753267952272
O	4.14396613775119	2.84447430108600	1.08955212621328
O	4.70726746554199	3.17650663582398	-1.53782971914616
Cl	5.09644882835872	5.77957665306195	0.26491936510856
Cl	2.58914496421611	5.60830544286013	-2.19594825656832
Cl	1.82753206066509	5.16186456844314	1.39651190636042
Cl	1.65759970508673	2.48687935014829	-0.87757127057371
Cl	9.39455773020883	-5.78090924713054	-0.26594396571801
Cl	11.90010500390006	-5.60637481127512	2.19648273201604
Cl	12.66333039431271	-5.15796978486666	-1.39536652582686
Cl	12.82768094846876	-2.48318184613882	0.87940332749786

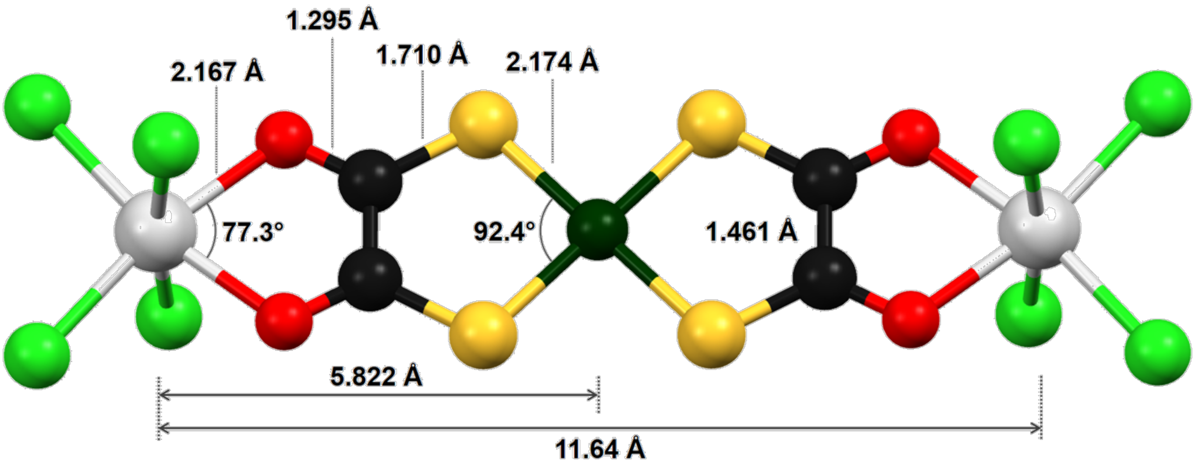

Fig. S13 Metrics for the optimised structure of $[Ni\{(dto)SnCl_4\}_2]^{3-}$

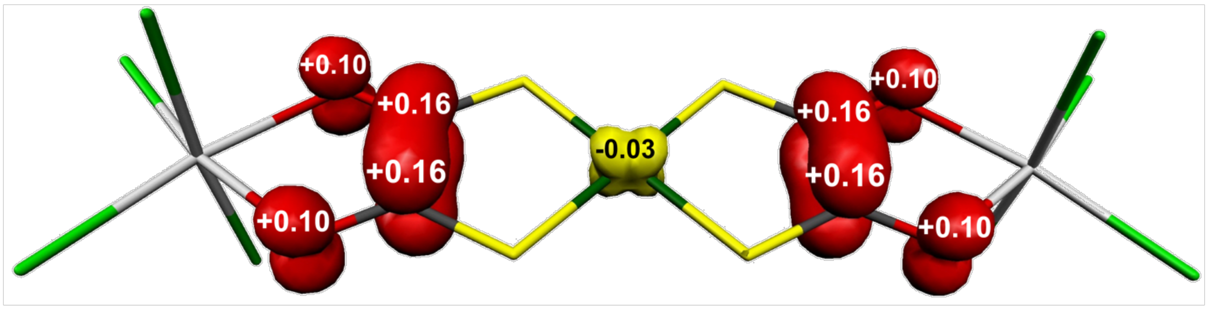

Fig. S14 Mulliken spin population analysis for $[Ni\{(dto)SnCl_4\}_2]^{3-}$ (red: α-spin; yellow: β-spin)

Table S3 Total Energies and Exchange Couplings from BS Calculations

		M_S	Spin Arrangement	Total Energy / E_h	J_{calcd} / cm^{-1}
2	BS(7,7)	7	↑↑↑↑↑↑↑ ↑↑↑↑↑↑↑	-29435.25132341	+0.02
		0	↑↑↑↑↑↑↑ ↓↓↓↓↓↓↓	-29435.25131849	
4	BS(14,1)	$^{15}/_{2}$	↑↑↑↑↑↑↑ ↑ ↑↑↑↑↑↑↑	-29434.71500317	-1.23
		$^{13}/_{2}$	↑↑↑↑↑↑↑ ↓ ↑↑↑↑↑↑↑	-29434.71508175	
	BS(8,7)	$^{15}/_{2}$	↑↑↑↑↑↑↑↑ ↑↑↑↑↑↑↑	-29434.71500480	+477.71
		$^{1}/_{2}$	↑↑↑↑↑↑↑↑ ↓↓↓↓↓↓↓	-29434.59307375	
	BS(7,6)	$^{13}/_{2}$	↑↑↑↑↑↑↑↓ ↑↑↑↑↑↑↑	-29434.71508126	+629.34
		$^{1}/_{2}$	↓↓↓↓↓↓↓↑ ↑↑↑↑↑↑↑	-29434.59459394	

References

1. R. B. King, F. G. A. Stone, W. J. Jolly, G. Austin, W. Covey, D. Rabinovich, H. Steinberg and R. Tsugawa, *Inorg. Synth.*, 1963, **7**, 99.
2. H. O. Jones and H. S. Tasker, *J. Chem. Soc., Trans.*, 1909, **95**, 1904.
3. P. Román, J. I. Beitia, A. Luque and C. Guzmán-Miralles, *Polyhedron*, 1995, **14**, 1091.
4. G. M. Sheldrick, *Acta Crystallogr. Sect. A*, 2008, **64**, 112.
5. G. M. Sheldrick, *Acta Cryst.*, 2015, **C71**, 3.
6. O. V. Dolomanov, L. J. Bourhis, R. J. Gildea, J. A. K. Howard and H. Puschmann, *J. Appl. Cryst.*, 2009, **42**, 339.
7. L. J. Farrugia, *J. Appl. Cryst.*, 1999, **32**, 837.
8. R. C. Clark and J. S. Reid, *Acta Crystallogr. Sect. A*, 1995, **51**, 887.
9. G. R. Hanson, K. E. Gates, C. J. Noble, M. Griffin, A. Mitchell and S. Benson, *J. Inorg. Biochem.*, 2004, **98**, 903.
10. F. Neese, *WIREs Comput. Molec. Sci.*, 2012, **2**, 73.
11. (a) A. D. Becke, *J. Chem. Phys.*, 1988, **84**, 4524. (b) J. P. Perdew, *Phys. Rev. B*, 1986, **33**, 8822.
12. S. Grimme, J. Antony, S. Ehlrich and H. Krieg, *J. Chem. Phys.*, 2010, **132**, 154104.
13. (a) A. Klamt and G. Schüürmann, *J. Chem. Soc., Perkin Trans. 2*, 1993, 799. (b) A. Klamt, *J. Phys. Chem.*, 1995, **99**, 2224. (c) A. Klamt and V. Jonas, *J. Chem. Phys.*, 1996, **105**, 9972.
14. (a) D. A. Pantazis and F. Neese, *J. Chem. Theory Comput.*, 2009, **5**, 2229. (b) F. Weigend and R. Ahlrichs, *Phys. Chem. Chem. Phys.*, 2005, **7**, 3297.
15. (a) J. P. Perdew, K. Burke and M. Ernzerhof, *Phys. Rev. Lett.*, 1996, **77**, 3865. (b) J. P. Perdew, K. Burke and M. Ernzerhof, *Phys. Rev. Lett.*, 1997, **78**, 1396. (c) C. Adamo and V. Barone, *J. Chem. Phys.*, 1999, **110**, 6158.
16. (a) R. Izsák and F. Neese, *J. Chem. Phys.*, 2011, **135**, 144105. (b) F. Neese, F. Wennmohs, A. Hansen and U. Becker, *Chem. Phys.*, 2009, **356**, 98.
17. (a) E. van Lenthe, J. G. Snijders and E. J. Baerends, *J. Chem. Phys.*, 1996, **105**, 6505. (b) E. van Lenthe, A. van der Avoird and P. E. S. Wormer, *J. Chem. Phys.*, 1998, **108**, 4783. (c) J. H. van Lenthe, S. Faas and J. G. Snijders, *Chem. Phys. Lett.*, 2000, **328**, 107.

18. C. J. van Wüllen, *J. Chem. Phys.*, 1998, **109**, 392.

19. P. Pulay, *Chem. Phys. Lett.*, 1980, **73**, 393. (b) P. Pulay, *J. Comput. Chem.*, 1982, **3**, 556.

20. (a) L. Noodleman, *J. Chem. Phys.*, 1981, **74**, 5737. (b) L. Noodleman, D. A. Case and A. Aizman, *J. Am. Chem. Soc.*, 1988, **110**, 1001. (c) L. Noodleman and E. R. Davidson, *Chem. Phys.*, 1986, **109**, 131. (d) L. Noodleman, J. G. Norman, J. H. Osborne, A. Aizman and D. A. Case, *J. Am. Chem. Soc.*, 1985, **107**, 3418. (e) L. Noodleman, C. Y. Peng, D. A. Case and J. M. Monesca, *Coord. Chem. Rev.*, 1995, **144**, 199.

21. (a) K. Yamaguchi, Y. Takahara and T. Fueno, in *Applied Quantum Chemistry*, ed. V. H. Smith, Reidel, Dordrecht, The Netherlands, 1986, p. p. 155. (b) T. Soda, Y. Kitagawa, T. Onishi, Y. Takano, Y. Shigetu, H. Nagao, Y. Yoshioka and K. Yamaguchi, *Chem. Phys. Lett.*, 2000, **319**, 223.

22. *Molekel*, Advanced Interactive 3D-Graphics for Molecular Sciences, Swiss National Supercomputing Center. https://ugovaretto.github.io/molekel/